**Aalborg Universitet**



# Power Quality Enhancement and Power Management of a Multi-Functional Interfacing Inverter for PV and Battery Energy Storage System

Mousazadeh, Seyyed Yousef ; Jalilian, Alireza; Savaghebi, Mehdi; Guerrero, Josep M.

# Power Quality Enhancement and Power Management of a Multi-Functional Interfacing Inverter for PV and Battery Energy Storage System

Seyyed Yousef Mosazade Mousavi [a], Alireza Jalilian [a,b] (Corresponding author), Mehdi Savaghebi[c], and Josep M. Guerrero[c]

s_y_mosazade@iust.ac.ir, jalilian@iust.ac.ir, mes@et.aau.dk, , joz@et.aau.dk

[a] Department of Electrical Engineering Iran University of Science and Technology

[b] Center of Excellence for Power System Automation and Operation, Iran University of Science and Technology

[c] Department of Energy Technology, Aalborg University, Denmark

Abstract: *In this paper, the control of an interface inverter for application of in a hybrid Photovoltaic (PV) and Battery Energy Storage System (BESS) is proposed. The control system of the inverter consists of two parts including power quality enhancement and active power control. A control approach for Battery State of Charge (SOC) and power management is proposed for improving the performance of BESS and load leveling purpose. Furthermore, in order to prevent the BESS from frequently charge and discharge during a day, the discharge of it can be can be controlled by operator or Microgrid central controller. The power quality enhancement function of the proposed method mitigates the effect of the unbalance and nonlinear loads within the microgrid on the three phase 4-wire grid. The simulation results show that by using the multifunctional inverters, the unbalance and harmonics of the loads are compensated; furthermore, the neutral current which is drawn from the grid is competently compensated. The simulation results show that by using the proposed power management system the load leveling and charge and discharge*

*management of battery energy storage considering the battery limitation for the sake of extending the battery service life are achieved.*

## 1. Introduction

In recent years, Renewable Energy Sources (RES) such as Photovoltaic (PV) and wind systems attract more attention rather than fossil fuel based ones because of environmental pollution and extinction of the conventional fuels [1-3]. The cost of PV modules and their power electronics devices have been decreased in recent years, while their efficiency has increased leading to more investment in their installation [1]. Different Maximum Power Point Tracking (MPPT) methods such as Perturb and Observe (P&O), Incremental Conductance (INC), fuzzy system have been proposed [4] in order to increase the efficiency of the system.

Due to uncertainty and intermittent nature of PV systems, energy storage systems can be used to compensate the power fluctuation delivered to the grid [5], [6]. The Battery Energy Storage System (BESS) which is considered as a mature technology is used for the management of the power delivered by PV systems. In the hybrid system of PV and BESS, power management system is based on State of Charge (SoC) of the battery and consumed power of the local load of MG [6].

On the other hand, the proliferation of nonlinear and unbalanced loads has made power quality a major concern in microgrids and distribution systems [7-8]. Active and passive power filters have been proposed for mitigation of problems related power quality [9-12]. Active filters do not have the drawbacks of passive filters such as bulkiness, fixed tuning

and resonance problems [9]. The main component of active filters is the inverter which is also applied for integration of PVs and BESSs to the grids. The concept of using multi-functional inverters has been suggested by some researchers. In this concept, not only the generated power of distributed generator (DG) can be injected to the grid or microgrid via proper control of inverter but also compensation of nonlinear and unbalanced loads effects can be achieved [13-20]. In [13-19], the DG units are not modeled and a constant DC source is used as DG units.

An investigation on combined operation of active power filter and photovoltaic arrays is presented in [20]. The investigation is applied on a three-wire three-phase inverter without considering management system. In [21], the multifunctioning of a BESS's inverter is proposed in a 4-wire three-phase system with nonlinear loads. The main aim of the method proposed in [21] is power quality compensation; however the control of charge and discharge of BESS is not presented.

A simple method for power management and control of multifunctional grid tied inverter of hybrid PV and BESS in 4-wire three-phase system is also presented in [22]. The power management system is simple and the limitation of BESS in charge and discharge is not considered. Furthermore, load leveling is another function of BESS which are not taken in to account in [22.]

In this paper, the power management system of [22] is improved in order to manage the charging and discharging of the BESS and load leveling purpose. The grid-tied inverter not only can support the active power of nonlinear and unbalanced loads in three phase 4-wire system but can also compensate the harmonics and unbalanced components of these loads. Furthermore, compensation of zero sequence and resulting neutral current of these loads is

obtained. The PV system is implemented based on MPPT method by using Adaptive Neuro-Fuzzy Inference System (ANFIS) maximum power estimation and a boost DC/DC converter. The number of charging and discharging cycles is an important factor; hence, the command signal which is called hereafter "Discharging order" is used for reducing the charging and discharging cycles which it not considered in [21, 22]. The discharging order can be generated by microgrids central controller or distribution system operator for economic or peak shaving purpose in smart grid. A power management algorithm considering SoC, load power and discharging order is applied to the system. The power management system can control the injected power of the hybrid system and consumption of loads. The main contribution of the paper can be summarized as follow:

- Power quality compensation by three phase 4-wire interfacing inverter of a hybrid battery and BESS

- Proposing a power management system based on local power consumption and SoC of the battery for the hybrid BESS and PV system.

- Control of the power absorbed from the grid and providing a control for microgrids central controller or distributed system operator in smart grid.

Rest of the paper is presented as follows:

In Section 2, the overall scheme of the system is presented. The control of the multifunctional system and applied power management system is described in Section 3. The simulation results and discussion are presented in Section 4 and finally the paper is concluded in Section 5.

## 2. General overview of the system

Fig. 1 shows the control and power stages of the system. As shown in the power stage,

hybrid PV and battery energy storage are connected to the grid by a three phase 4-leg

inverter while the PV is connected via a DC/DC boost converter to the BESS in DC link.

Single and three phase nonlinear and unbalanced loads are considered as local load in this

study. The control system consists of DC/DC and DC/AC converter control. The reference

active power of the DG ($P_{ref\_DG}$) is generated by power management system



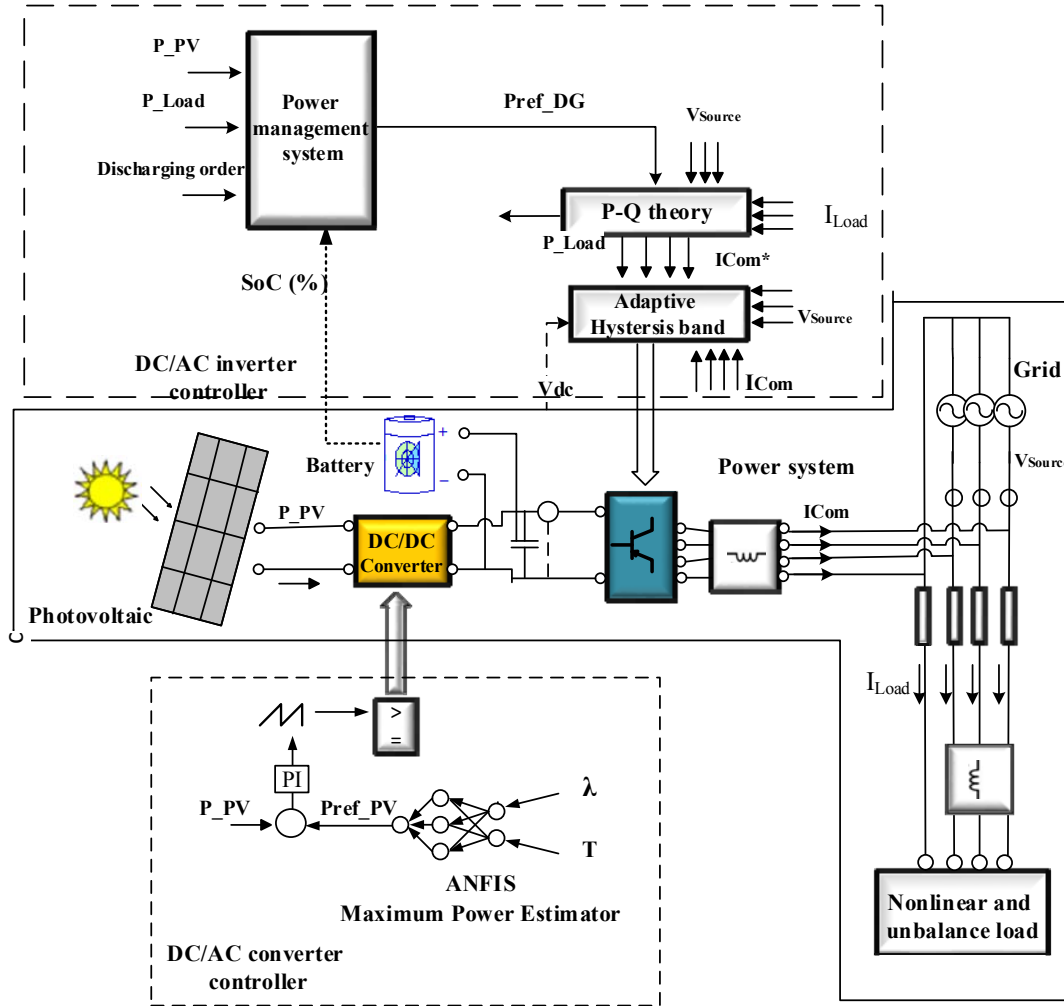Fig.1- Power and control stages of the simulated system

which controls the injected power to the grid and SoC of the battery. The instantaneous

reactive power (p-q) theory is used for harmonics and unbalanced load compensation. The

calculated active power of load is also used in power management system. The power

injected in load feeder is considered as load power and the load feeder loss is not

considered. However, since the load feeder current is measured, the load feeder loss power can be calculated if the parameters of feeder are available. For solving the drawback of conventional hysteresis band controller, adaptive hysteresis band controller is used to generate pulse signals for the inverter.

## 2.1. PV and MPPT systems

The power which is generated by PV system is in DC form. The equivalent circuit of a PV module is depicted in Fig.2. In this figure, photo current, internal resistance and parallel leakage resistance are presented by $I_{PV}$, $R_S$ and $R_{SH}$, respectively. $N_s$ and $N_P$ represent the number of series and parallel cells.

The current versus voltage equation is expressed using equation (1):

$$I = I_{PV} - I_0 \left[ \exp(\frac{V + R_S.I}{V_t m}) - 1 \right] - \frac{V + R_S.I}{R_S}$$

(1)
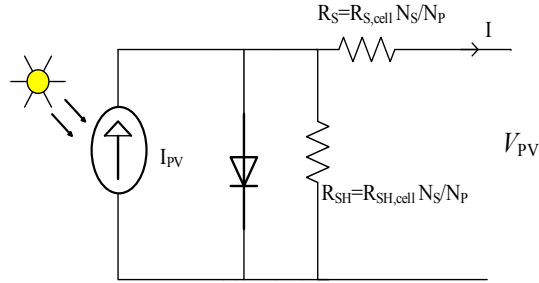


Fig.2 Equivalent circuit for a PV array

where $I_{PV}$ and $I_0$ represent the photovoltaic and saturation currents of the PV array, respectively. Considering $k$, $q$, $T$, $N_S$ as Boltzmann's constant of the diode, electron charge, temperature of the module, and number cells connected in series, respectively, the thermal voltage can be calculated by $V_t = N_s.k.T/q$. With the connection of the $N_p$ numbers of PV cells in parallel, the photovoltaic and saturation currents of PV array can be written as:

$I_{PV} = N_P.I_{PV,cell}$, $I_0 = N_P.I_{0,cell}$

(2)

The photovoltaic current generated by the semiconductor device is changed in different temperatures and sun irradiance. Equation (3) describes the relation between photovoltaic current, temperature and solar irradiance.

$$I_{PV} = (I_{PV,n} + K_I \Delta T) \frac{G}{G_n}$$

(3)

where $I_{PV,n}$ is the photovoltaic current in standard 25° C and 1000 W/m$^2$ solar irradiance. $K_I$ is the temperature coefficient of short circuit current. The sun irradiance and the nominal irradiation are also represented by $G$ and $G_n$ in this equation. $\Delta T = T - T_n$ is the deference of actual ($T$) and nominal temperatures ($T_n$) in kelvin.

The saturation current ($I_0$) also depends on the temperature. The following equation expresses the dependency:

$$I_0 = I_{0,n} \left( \frac{T_n}{T} \right)^2 \exp \left[ \frac{q E_g}{ak} \right] \left( \frac{1}{T_n} - \frac{1}{T} \right)$$

(4)

where $I_{0,n}$ and $E_g$ represent the nominal saturation current and band gap energy of semiconductor at 25° C. Table.1 shows the characteristic of the simulated PV array [23].

Table.1 -Sample parameters of a PV system for modeling and illustration.

| Definition | Symbol | Value |
|---|---|---|
| Number of series cells | $N_S$ | 1200 |
| Number of parallel cells | $N_P$ | 12 |
| Temperature coefficient | $K_I$ | 0.03 |
| Open circuit voltage at normal temperature | $V_{OC}$ | 1200×0.6=720 V |
| Short circuit current | $I_{SC}$ | 12×3.6=43.2 A |
| Reference Temperature | $T_{ref}$ | 25° C |
| Shunt resistance | $R_{SH,cell}$ | 10 kΩ |
| Series resistance | $R_{S,cell}$ | 10 µΩ |
| Ideal factor of solar cells | m | 3.3 |

2.2.    Maximum power tracking system

DC/DC boost converters have been proposed by researchers for MPPT purpose, since, these converters not only can track MPP, but also can boost the voltage of the PV [4].

In this paper, an ANFIS algorithm is used as estimator in the MPPT process. In this method, a trainable multi-layer network that integrates the characteristics of Surgeon fuzzy systems is used with multi-layer feed forward adaptive neural networks features.

Fig.3 shows the data set which is used for training purpose of the adaptive Neuro-fuzzy inference system. The data set is obtained by simulation of the PV with the parameters listed in Table.1, in different temperature and sun irradiance.

ANFIS method is employed to model the nonlinear functions and detect the inner nonlinear behavior of solar cells, in order to calculate the maximum power of PV in different temperatures and irradiations [24].
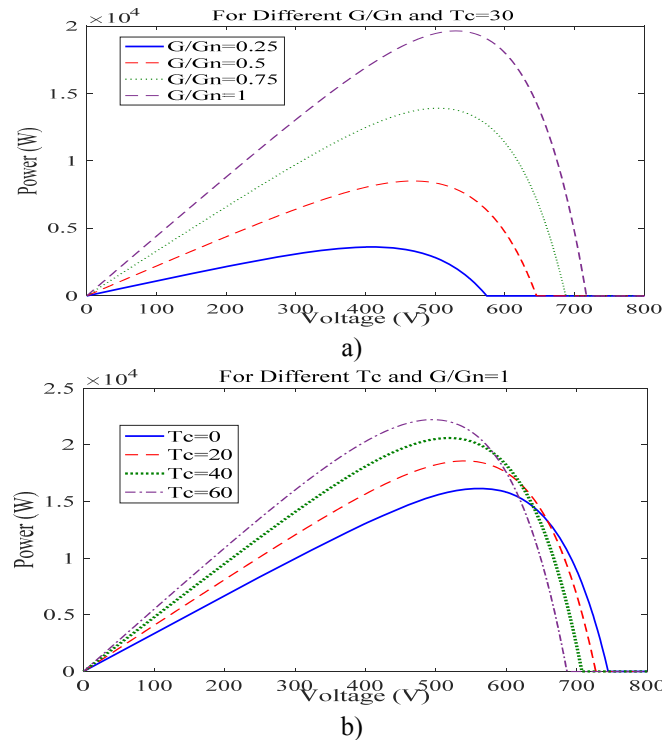


Fig. 3, PV P-V curves charactristic
a-changing the maximum power in different sun irradiance and Tc=30
b-changing the maximum power in different temperature and G/G$_n$=1

ANFIS is an adaptive and trainable multi-layer network. The most important advantages of ANFIS in comparison to other conventional systems are fast and accurate learning besides fine tuning of membership functions [25, 26]. The typical structure of ANFIS is shown in Fig.4 which contains 5 distinct layers. For generating initial fuzzy interface system, Grid partition, subtractive clustering, FCM clustering following three classification methods are usually used [27].



Fig. 4     ANFIS Structure
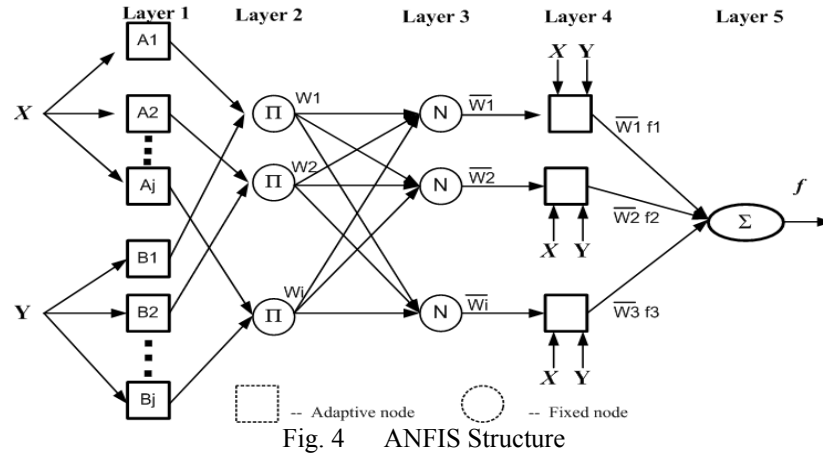
The control block of DC/DC converter is depicted in Fig.1. In this figure, $P_{ref\_PV}$ represents the reference power which is 90% of maximum power estimated by MPPT system (with the assumption of 10% security margin) [28].

2.3. Battery energy storage

Lead acid batteries can be used as technical feasible, economically viable and sustainable BESS technology in utility application such as spinning reverse, load following, frequency control, load leveling [29, 30]

The lead acid battery model used in [28] is simulated in this paper. This model is based on two internal resistances for charge and discharge states. The values of these resistances and internal voltage of battery are dependent on battery SoC; hence, the output voltage and

resistances should be defined based on SoC.

SoC is one of the most important signals used for battery control and it is defined as [28]:

$$SoC = \frac{A.h - Ah_{used}}{A.h} \tag{5}$$

$$Ah_{used} = Ah \times (1 - SoC_{(0)}) + \int \frac{I_b}{3600} dt \tag{6}$$

$$I_b = \frac{V_{oc} - \sqrt{4R_{int} \cdot P_{el}}}{2R_{int}} \tag{7}$$

where $A.h$, $Ah_{used}$, $P_{el}$, $V_{OC}$ and $R_{int}$ represent battery nominal capacity, battery used capacity, battery output power, battery open circuit voltage and internal resistance, respectively. are The parameters of the simulated battery energy storage are listed in Table.2.

Table.2- Parameters of the battery energy storage

| Parameter | Symbol | Value |
|---|---|---|
| Number of series | $N_b$ | 63 |
| Capacity | A.h-Cap | 100 A.h |
| Open circuit voltage | $V_{oc}$ | 12×63=756 |

3-Control of the inverter and power management system

3.1. Power management system

The reference power of the DG ($P_{ref\text{-}DG}$) is determined from SoC of battery, PV generated power, local load power and "Discharging order". Fig. 6 shows the reference power generation of the proposed power management system. In the first step, the data gathered by the measuring instrument is updated. In the second step, the PV generated power ($P_{PV}$) is compared with the local load of the microgrid. If the amount of the generated power is higher than the local load, battery works in charging mode and the reference power of

inverter will be $P_{ref\text{-}DG} = K_1 . P_{PV}$. The amounts of $K_1$ are listed in Table.3. Note that the upper limit of SoC=100% and if the SOC reaches the limit, the reference power of DG will be equal to $P_{PV}$ and the BESS will be inactive. As shown in this table, for low amount of the SoC, the amount of $K_1$ is lower, since the battery should be charged faster. In other words, by using the low amount of $K_1$ the injected power of the DG to grid is lower and the battery will be charged by absorbing the power of PV.

In order to limit the maximum demand of the local load, the power received by the local load from the grid ($P_{load} - P_{PV}$) is monitored. If the power is lower than the maximum demand ($P_{critical}$), a power in the amount of $P_{load} - P_{critical}$ will be injected to the grid by the inverter ($P_{ref\text{-}DG} = P_{load} - P_{critical}$). If the power is more than maximum demand, the "Discharging order" is checked. The discharging order may be controlled by economical calculation or microgrid controller and is used for preventing the battery form charging and discharging frequently in a day. If the amount of "Discharging order" is 1, the battery will be operating in discharging mode and the reference power is ($P_{ref\text{-}DG} = P_{PV} + K_2 . P_{rated}$). $P_{rated}$ denotes the nominal power of PV system. The amounts of $K_2$ are listed in Table 4.

If the discharging order is 0, the injected power of the inverter will be equal to the generated power of the PV ($P_{ref\text{-}DG} = P_{PV}$). In other words, the BESS will be inactivated in this mode. It should be mentioned that the depth of discharge of the battery is monitored in discharging mode and the lower allowable limit of SoC is assumed to be 20% in this paper.
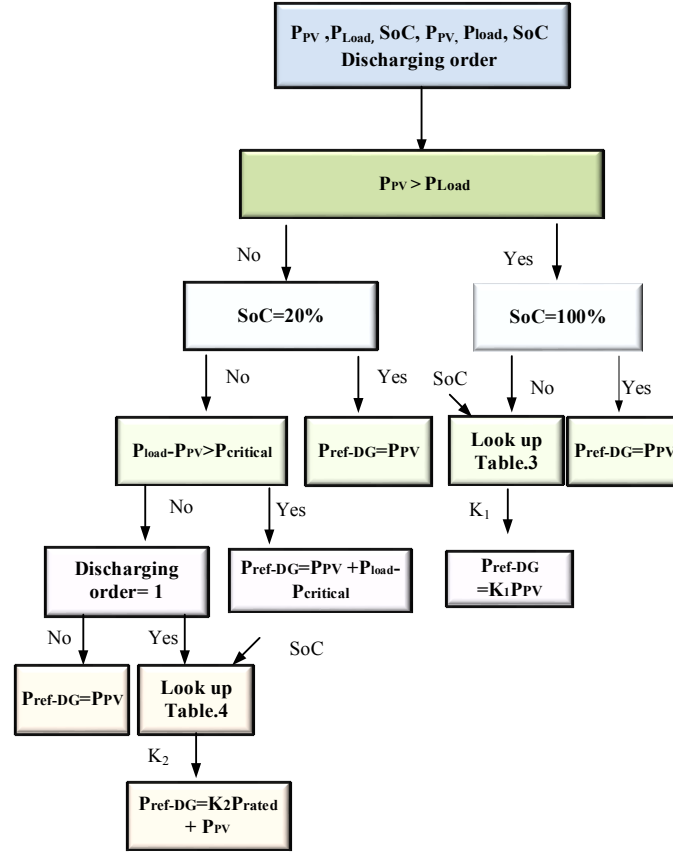
Fig.5. the power management system

Table.3- $K_1$ coefficient of injected power to grid in charging mode

| SOC (%) | 20 | 30 | 40 | 50 | 60 | 70 | 80 | 100 |
|---------|----|----|----|----|----|----|----|-----|
| $K_1$ | | 0.5 | 0.65 | 0.75 | 0.825 | 0.875 | *0.925* | 0.975 | 1 |

Table.4- $K_2$ coefficient of injected power to grid in charging mode

| SOC (%) | 20 | 30 | 40 | 50 | 60 | 70 | 80 | 100 |
|---------|----|----|----|----|----|----|----|-----|
| $K_2$ | 0 | .25 | .45 | .6 | 0.75 | 0.85 | 1 | 1.2 |

## 3.2. Multifunctional control of grid-tied inverter

As aforementioned, in this paper multifunctional control of grid tied inverter as a power quality compensator and DG power conditioner is presented. The control is implemented using instantaneous reactive power (p-q) theory in three phase 4-wire system. In p-q theory, firstly three phase voltage and current should be converted to α-β-0 [31].

The instantaneous real and imaginary power can be written as:

$$\begin{bmatrix} p \\ q \\ p_0 \end{bmatrix} = \begin{bmatrix} V_\alpha & V_\beta & 0 \\ -V_\beta & V_\alpha & 0 \\ 0 & 0 & V_0 \end{bmatrix} \begin{bmatrix} i_\alpha \\ i_\beta \\ i_0 \end{bmatrix}$$

(7)

where $p$ and $q$ represent instantaneous real and reactive power, respectively; furthermore, the zero sequence real power is represented by $p_0$. These instantaneous real and imaginary powers contain two dc and oscillation parts as (8):

$$p = \bar{p} + \tilde{p}$$
$$q = \bar{q} + \tilde{q}$$
$$p_0 = \bar{p}_0 + \tilde{p}_0$$

(8)

where $\bar{p}$, $\bar{q}$ and $\bar{p}_0$ correspond to DC part of real and imaginary powers. $\tilde{q}$, $\tilde{p}$ and $\tilde{p}_0$ represent the oscillation parts of these powers.

$\bar{q}$ is the conventional fundamental positive sequence reactive power and can be compensated by the multifunctional system. The oscillation terms of powers are related to harmonics and unbalanced condition; hence, the part of power which should be compensated. For compensation of neutral current both $\tilde{p}_0$ and $\bar{p}_0$ should be compensated.

In order to inject the reference power of DG to the grid and harmonics and unbalance compensation, the reference current is expressed as following equation by reversing of (7) [22]:

$$\begin{bmatrix} i_\alpha \\ i_\beta \\ i_0 \end{bmatrix} = \frac{1}{\left(V_\alpha^2 + V_\beta^2\right)V_0} \begin{bmatrix} V_\alpha V_\beta & -V_0 V_\beta & 0 \\ V_0 V_\beta & V_0 V_\alpha & 0 \\ 0 & 0 & V_\alpha^2 + V_\beta^2 \end{bmatrix} \begin{bmatrix} P_{ref-DG} + \tilde{p} \\ \bar{q} + \tilde{q} \\ p_0 \end{bmatrix}$$

(9)

The reference signal in α-β-0 should be converted to a-b-c frame. Afterwards, these reference currents are compared to real a-b-c frame currents and according to the hysteresis band switching method, proper pulses for IGBT switches are obtained. The hysteresis band

controller is presented in [31] and described in the next section.

## 3.3. Interfacing inverter and switching method

For injecting the zero sequence current to the four-wire grid with the aim of compensation, three common ways including zigzag or a delta-star transformer, three-leg split-capacitor structure and three phase four-leg topology have been suggested. Incorporation of zigzag or delta-star transformer is costly and bulky, since a fundamental frequency transformer is required in this solution. Although the use of split-capacitor solution is both easier and cheaper, injection of zero sequence current may cause dc voltage imbalance between the two splitting capacitor. In this paper, a three phase 4-wire 2-level inverter which is depicted in Fig.6 is used for injecting current to the grid [32].
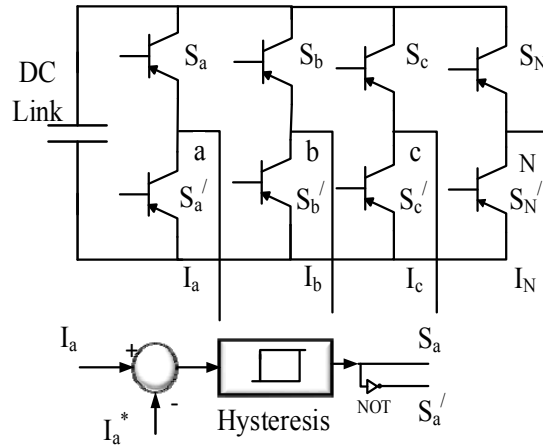


Fig.6- Four-leg inverter

As shown in this figure, for each phase, the reference and actual values ($I_a$ and $I_a{}^*$ for phase $a$) of the current are compared and the switching pulses of IGBT switches are generated according to the following logical function [31]:

$$\begin{cases} if \quad I_a - I_a^* > HB \qquad S_a = 1, S_a' = 0 \\ f \quad I_a - I_a^* < HB \qquad S_a = 0, S_a' = 1 \end{cases}$$

(10)

where *HB* represents the hysteresis band. The low amount of *HB* cause an increment in the

frequency of the inverter high while high amount of it leads to high current error. Although, the conventional hysteresis band controller has some advantages such as simplicity, fast dynamic response and limiting peak current, switching frequency is variable due to the use of fixed *HB*. For removing this drawback, adaptive hysteresis band controller is proposed in [31]. In this method, the *HB* is changed in a period in order to fix the switching frequency. In this paper, the adaptive hysteresis band controller which is proposed in [31] is applied to the three phase inverter. The adaptive hysteresis band is expressed by (10) [31].

$$HB = \left\{ \frac{0.125 V_{dc}}{f_c L} \left[ 1 - \frac{4L^2}{V_{dc}^2} \left( \frac{v_s}{L} + m \right)^2 \right] \right\}$$
(11)

where $V_{dc}$, $f_c$, $L$, $m$ represent the DC link voltage, switching frequency, link inductor and rate of current (di/dt) of DG interfacing inverters, respectively.

5.    Simulation results

The system shown in Fig.1 is considered as a simulation case study. The PV and battery parameters are available in Tables 1 and 2, respectively. The parameters of the grid-tied inverter and power system are listed in Table 5. The unbalanced and nonlinear loads are modeled as three and single-phase uncontrolled diode-bridge rectifiers. Two scenarios which are described in the following sections are applied to the system.

Table 5- parameters of the simulation

| | |
|---|---|
| ***Average Switching frequency*** | ***12 kHz*** |
| Fundamental frequency | 60 Hz |
| AC supply phase voltage | 230 V |
| Load side inductance | 1mH |
| Inverter side inductor | 3mH |
| Dc link capacitor | 10 mF |
| $P_{critical}$ | 3 kW |
| $P_{Rated}$ | 10kW |

A.    Scenario I

In the first scenario, the following steps are used:

- Step I: At t=.06s the hybrid PV and BESS system is connected to the DC link. The initial temperature, SoC, and sun irradiance are considered as 30° C, 20% and 1 kW/m2, respectively.

- Step II: After t=0.15s, the compensation part of the injected current is activated.

- Step III: to evaluate the effectiveness of the MPPT system, sudden change in sun
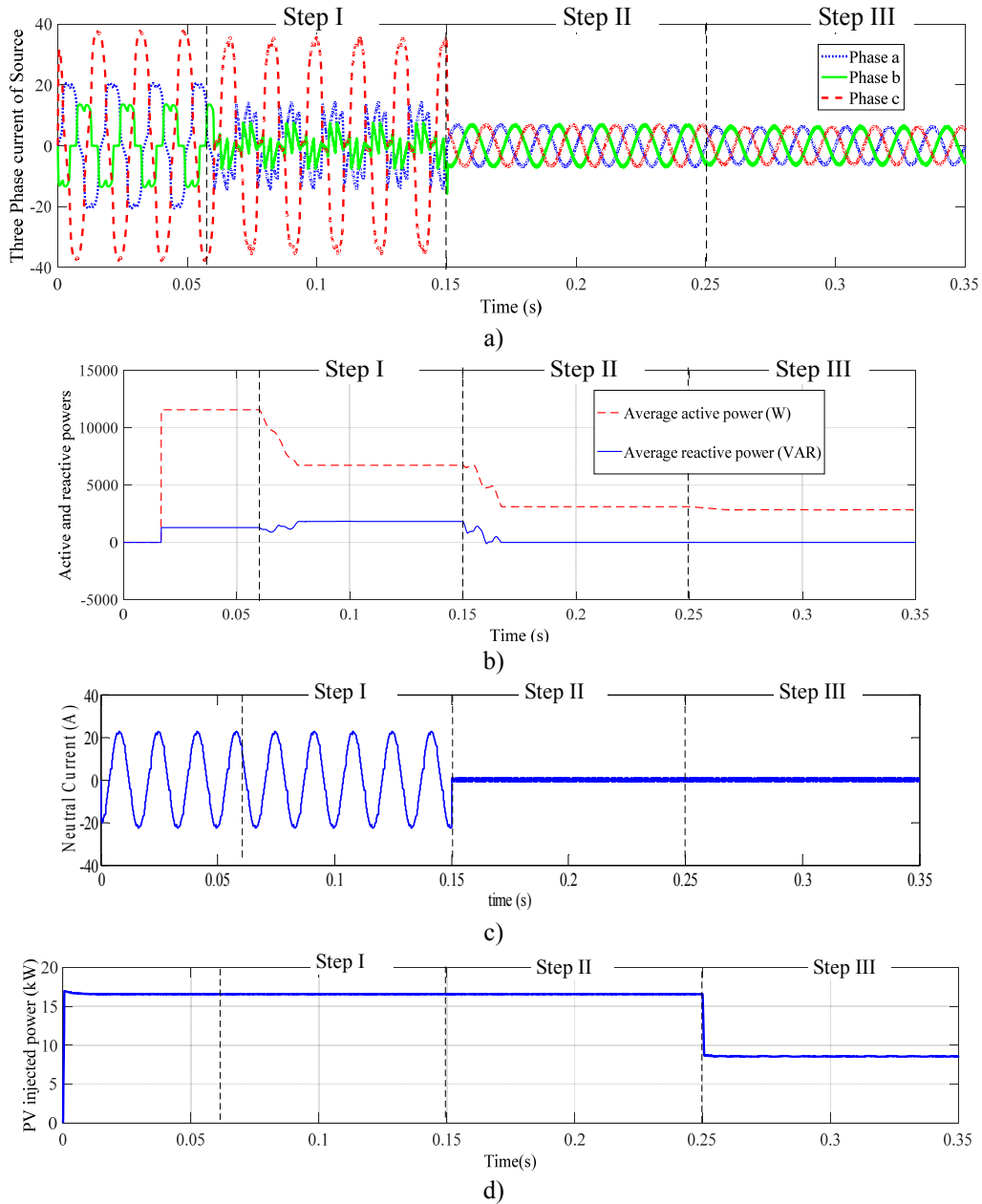


Fig.7 first scenario simulation : a) three phase current of source, b), average active and reactive current of source, c) neutral current, d) power generated by PV

Table.6- THD of grid current in first scenario

|  | Phase a | Phase b | Phase c |
|---|---|---|---|
| Step I | 31% | 35% | 17% |
| Step II | 3.97% | 3.8 % | 3.81% |
| Step III | 3.85% | 3.79 % | 3.76 |

irradiance to 0.6 kW/m$^2$ is exerted to the simulation at t=0.25s.

Fig. 7 shows the simulation results of this scenario. The grid source current is depicted in Fig. 7.a. As can be seen, after activation of harmonics and unbalance compensation, the grid source current is compensated. The values of current THD at different steps are listed in Table 6.

B.    Scenario II

In order to verify the effectiveness of PV and BESS energy management system, the simulation is implemented in different SoC (low SoC=20% and high SoC=80%) with variation of the generated PV power. In the first simulation, the initial SoC of the battery is considered to be 20% and following steps are applied in order to evaluate the effectiveness of the power management system

•    Step 1- low SoC and high PV power generation:

Firstly, the sun irradiance is considered as 1 kw/m$^2$ and the local load is 11.5 kW. In this condition, the amount of $P_{PV}$ is higher than the local load power; hence, the battery is in charging mode and is charged rapidly.

•    Step 2- low SoC and low PV power generation:

The sun irradiance is changed to 0.55 kw/m$^2$ at t=0.2s and the generated PV power is decreased. Since the absorbed power from the grid is higher than the critical load limit ($P_{load}$- $P_{PV}$ > $P_{critical}$ ), the SoC will be decreased to reach the depth of charge of 20% according to the power management system depicted in Fig. 5.

•    Step 3- changing active power of load.

In this step, the active power of load is decreased to 5150 W at t=0.4s. Since the PV generated power is higher that the load active power consumption, the BESS is charged according to the BESS power management system.

- Step 4- changing sun irradiance and temperature.

The sun irradiance changes to 0.8 kw/m$^2$ and the temperature changes from 30° C to 40° C at t=40s. Since the PV generated power increases in this step in comparison to Step 3; hence, the BESS is charged in higher rate in this step than Step 3. Fig. 8 shows the SoC, $P_{load}$, $P_{PV}$ and average injected power of the hybrid system to the grid.

At the second simulation, the initial SoC is assumed to be 80% and the following steps are used to show the effectiveness of the power management system:

- Step a: The initial sun irradiance is considered equal to 1 kW/m$^2$ and the power of local load is assumed to be 11.5 kw. According to the power management system, since the generated PV power is more than the load power, the battery should be charged in this condition.

- Step b: The sun irradiance is changed to 0.8 kW/m$^2$ at t=0.15s. In this condition, the injected power from the grid is lower than the critical power; thus, discharging of the battery energy storage is dependent on the "Discharging order" command. The aim of the "Discharging order" command is preventing the battery energy storage from charging and discharging for many times in a day which enhances the durability of the battery. Firstly, the discharging order is activated ("Discharging order" =1). In this condition, the amount of injected power of the hybrid system is more than the PV generated power and the BESS will be discharged.
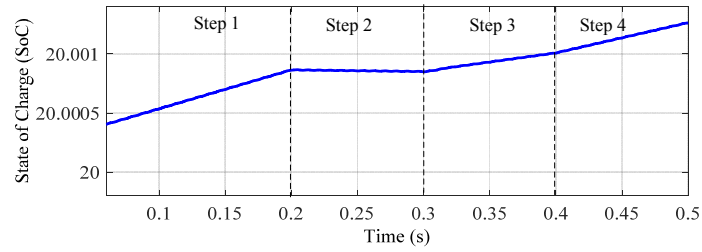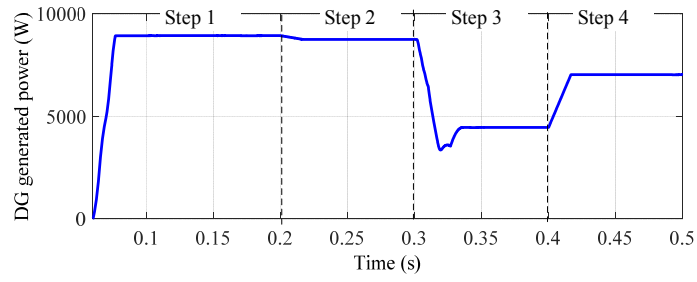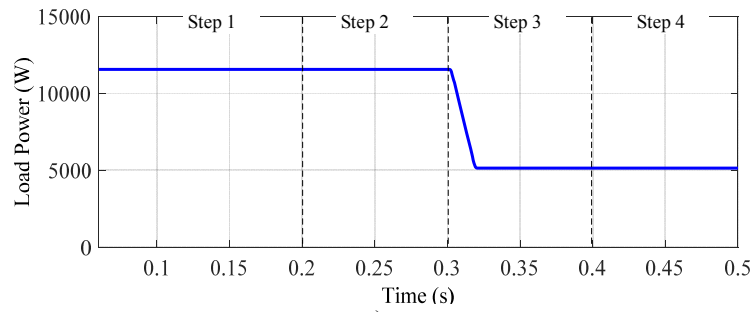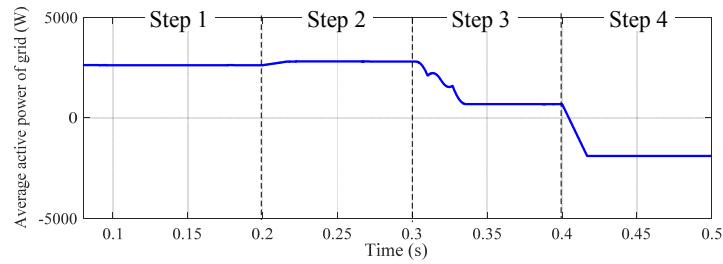
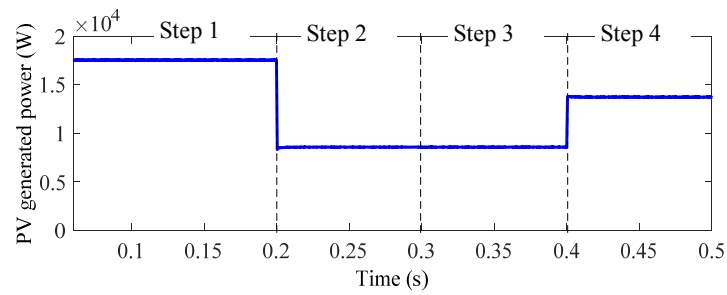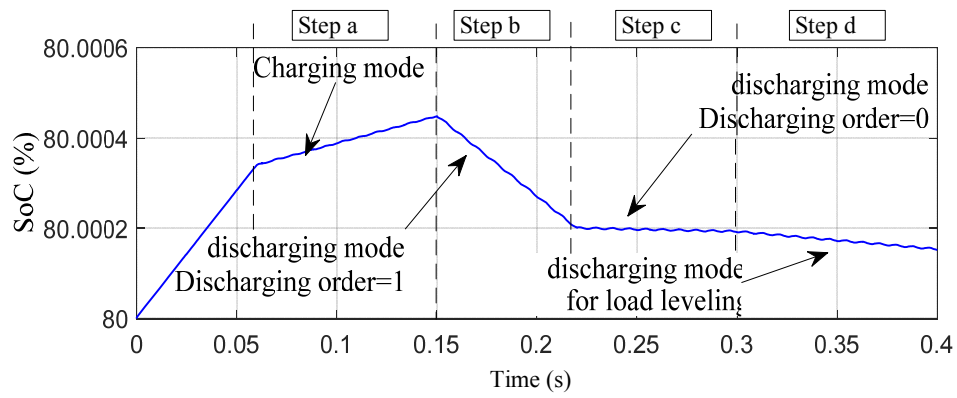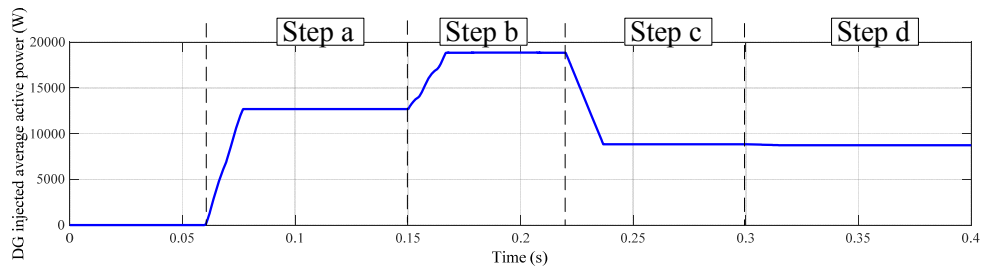Fig.8 .Simulation results in second scenario with initial SoC=20%, a –SoC, b-DG (hybrid system) power, c-Load power, d-grid active power , e- PV generated power

- Step c: At t= 0.22s the discharging is deactivated ("Discharging order =0"). In this mode, the power delivered by the interfacing inverter to the grid is equal to the PV generated power and the BESS is inactive.

  - Step d: In the last step of the simulation, at t=0.30 the sun irradiance decreases to 0.5 kW/m$^2$. Since, the injected power from the grid ($P_{load} - P_{PV}$) is more than the critical load; the battery will be discharged for load leveling purpose, although the "Discharging order" is 0. In other words, as it shows in the power management system (Fig. 5), the maximum injected power from the grid is limited by local measurement and is not dependent on the discharging order (load leveling is prioritized).
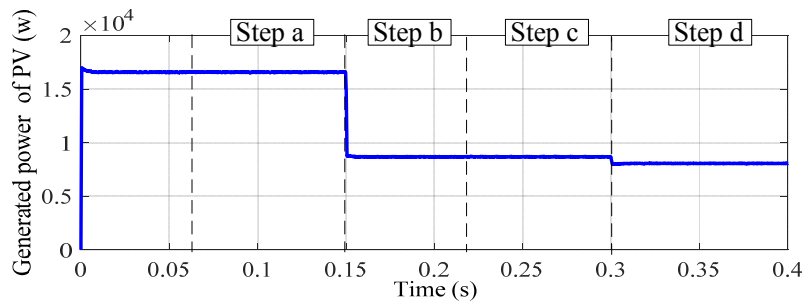
Fig. 9 shows the SoC, $P_{load}$, $P_{PV}$ and average injected power of the hybrid system to the grid in these steps.
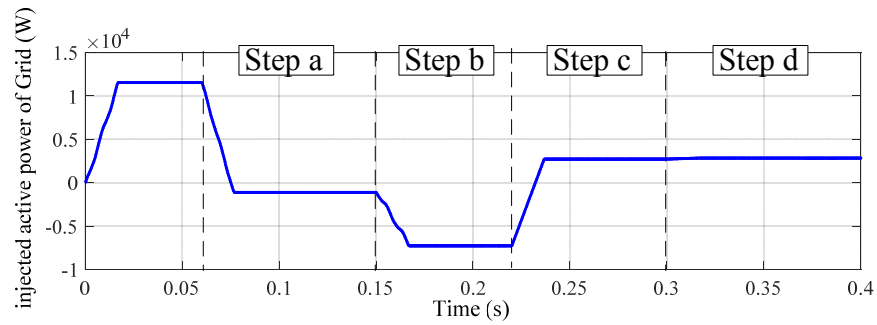
a)



b)



c)



d)

Fig,9 – Simulation results in second scenario with initial SoC=80%, a –SoC, b-DG generation, c-- PV

generated power, d-Source average active power

Conclusions:

In this paper, control of a multifunctional grid tied inverter for injecting the power of a hybrid battery energy storage and PV system and power quality enhancement is presented. The simulation results show that by using p-q algorithm, not only the power of the distributed hybrid energy resource can be delivered, but, also the power quality problems caused by local nonlinear and unbalanced loads can be solved.

Two scenarios are implemented in this paper. The first scenario is dedicated to the power quality aspect of the system while the second scenario is implemented for verifying the power management system. The simulation results of the first scenario show that after activation of compensation function of the inverter, the unbalance and harmonic current of the nonlinear and unbalanced local loads will be compensated. Furthermore, neutral current compensation is achieved by this approach. Moreover, effectiveness of the MPPT algorithm is validated by sudden change in sun irradiance. In the second scenario, simulation results show that the power management system has three advantages. The first advantage is that PV can charge the battery when the PV generated power is more than the critical active power. Additionally, the stored power in the battery is used for the purpose of load leveling when the injected power from the grid is higher than the critical load power. The other feature is that the discharging order is required which prevents the battery to charge and discharge for many times during a day. The remaining capacity of the BESS can be used by discharging order which can be sent by the operator or microgrid central controller.

**Symbols:**

$I_{PV}$ : photo current; $R_S$ : internal resistance; $R_{SH}$ : parallel leakage resistance; $I_0$ : saturation

currents of the PV; $k$ : Boltzmann's constant of the diode; $q$: Boltzmann's constant of the diode; $T$: temperature of PV module; $N_S$ : number cells connected in series; $N_p$ : numbers of PV cells in parallel; $I_{PV,n}$ : The photovoltaic current in standard 25° C and 1000 W/m$^2$ solar irradiance; $K_I$ : temperature coefficient of short circuit current; $G$ : actual sun irradiance; $G_n$ : nominal irradiation; $T_n$ : nominal temperatures in kelvin; $I_{0,n}$ : the nominal saturation current; $E_g$ : band gap energy of semiconductor at 25̊ C; $V_{OC}$ : Open circuit voltage of PV at normal temperature; $m$: Ideal factor of solar cells; SoC : state of charge; $N_b$ : Number of series battery; $A.h$ : battery nominal capacity; $Ah_{used}$ : battery used capacity; $P_{el}$ : battery output power; $P_{ref\text{-}DG}$ : reference power of the DG; $P_{PV}$ : PV generated power; $P_{load}$ : power of the local load; $P_{critical}$ : maximum demand; p : instantaneous real power; q : instantaneous reactive power; $\bar{p}$ : DC part of real power;

## Reference:

[1] Bose, B.K., "Global Warming: Energy, Environmental Pollution, and the Impact of Power Electronics," , IEEE Industrial Electronics Magazine, vol.4, no.1, pp.6,17, March 2010

[2] T.C. Green, M. Prodanović, "Control of inverter-based micro-grids," Electric Power Systems Research Vol.77, no.9, pp.1204–1213, 2007.

[3] Khederzadeh, Mojtaba, and Hamed Maleki. "Coordinating storage devices, distributed energy sources, responsive loads and electric vehicles for microgrid autonomous operation." International Transactions on Electrical Energy Systems 25, no. 10 (2015): 2482-2498.

[4] D B.C Chen; C.L Lin, "Implementation of Maximum-Power-Point Tracker for Photovoltaic Arrays, " Industrial Electronics and Applications (ICIEA), 2011 6th IEEE Conference, P.P.1621-1626,2011.

[5] Jimeno, Joseba, Jon Anduaga, José Oyarzabal, and Asier Gil de Muro. "Architecture of a microgrid energy management system." International Transactions on Electrical Energy Systems 21, no. 2 (2011): 1142-1158.

[6] Xiangjun, L. I., Y. A. O. Liangzhong, and H. U. I. Dong. "Optimal control and management of a large-scale battery energy storage system to mitigate fluctuation and intermittence of renewable generations." Journal of Modern Power Systems and Clean Energy 4.4 (2016): 593-603..

[7] S. Chowdhury, S.P. Chowdhury and P. Crossley, "Microgrids and Active Distribution Networks," 1th edition, IET Publisher, UK, 2009.

[8] An, L. U. O., et al. "Overview of power quality analysis and control technology for the smart grid." Journal of Modern Power Systems and Clean Energy 4.1 (2016): 1-9.

[9] H. Akagi and K. Isozaki , " A Hybrid Active Filter for a Three-Phase 12-Pulse Diode Rectifier Used as the Front End of a Medium-Voltage Motor Drive" IEEE transaction on power electronics, VOL. 27, NO,PP.69-77, January 2012.

[10] Singh, Bhim; Al-Haddad, K.; Chandra, A., "A review of active filters for power quality improvement," IEEE Transactions on Industrial Electronics vol.46, no.5, pp.960-971, Oct 1999.

[11] G Graovac, D.; Katic, V.; Rufer, A., "Power Quality Problems Compensation With Universal Power Quality Conditioning System," IEEE Transactions on Power Delivery, vol.22, no.2, pp.968-976, April 2007.

[12] Rahmani, B.; Tavakoli Bina, M., "Reciprocal effects of the distorted wind turbine source and the shunt active power filter: full compensation of unbalance and harmonics under 'capacitive non-linear load' condition," IET Power Electronics, vol.6, no.8, pp.1668-1682, September 2013.

[13] Zheng Zeng; Huan Yang; Shengqing Tang; Rongxiang Zhao, "Objective-Oriented Power Quality Compensation of Multifunctional Grid-Tied Inverters and Its Application in Microgrids," , IEEE Transactions on Power Electronics, vol.30, no.3, pp.1255,1265, March 2015.

[14] Shahnia, F., Majumder, R., Ghosh, A., Ledwich, G., Zare, F., "Operation and control of a hybrid microgrid containing unbalanced and nonlinear loads, " Electric Power Systems Research, vol.80, no.8,: pp. 954-965, 2010.

[15] Savaghebi, M.; Jalilian, A.; Vasquez, J.C.; Guerrero, J.M., "Autonomous Voltage Unbalance Compensation in an Islanded Droop-Controlled Microgrid," IEEE Transactions on Industrial Electronics, vol.60, no.4, pp.1390-1402, April 2013

[16] Jinwei He; Yun Wei Li; Blaabjerg, F., "Flexible Microgrid Power Quality Enhancement Using Adaptive Hybrid Voltage and Current Controller," IEEE Transactions on Industrial Electronics, vol.61, no.6, pp.2784-2794, June 2014.

[17] S. Y. Mousazadeh Mousavi, A. Jalilian, M. Savaghebi and J. M. Guerrero GE, "Autonomous Control of Current and Voltage Controlled DG Interface Inverters for Reactive Power Sharing and Harmonics Compensation in Islanded Microgrids," IEEE Transactions on Power Electronics, Early acess, 2018.

[18] Mousazadeh Mousavi, S.Y.; Jalilian, A.; Savaghebi, M.; Guerrero, J.M. "Flexible Compensation of Voltage and Current Unbalance and Harmonics in Microgrids" Energies 10, 1568, 2017,.

[19] S. Y. Mousazadeh Mousavi,, et al. "Coordinated control of multifunctional inverters for voltage support and harmonic compensation in a grid-connected microgrid." Electric Power Systems Research 155, pp. 254-264, 2018.

[20] Noroozian, R. and G.B. Gharehpetian, "An investigation on combined operation of active power filter with photovoltaic arrays " International Journal of Electrical Power & Energy Systems,. vol.46: p.p 392-399, 2013.

[21] Wasiak, I; Pawelek, R.; Mienski, R., "Energy storage application in low-voltage microgrids for energy management and power quality improvement," Generation, Transmission & Distribution, IET , vol.8, no.3, pp.463,472, March 2014.

[22] S. Y. Mousazadeh; M. Savaghebi, Beirami, A.; Jalilian, A; Guerrero, Josep M.; Li, Chendan, "Control of a multi-functional inverter for grid integration of PV and battery energy storage system," 2015 IEEE 10th International Symposium on Diagnostics Electrical Machines,Power Electronics and Drives (SDEMPED), pp.474-480, 1-4 Sept. 2015.

[23] M. G. Villalva, J. R. Gazoli, and E. R. Filho, "Comprehensive Approach to Modeling and Simulation of Photovoltaic Arrays," IEEE Trans. Power Electron., vol. 24, no. 5, pp. 1198–1208, May 2009.

[24] F. Khosrojerdi, S. Taheri and A. M. Cretu, "An adaptive neuro-fuzzy inference system-based MPPT controller for photovoltaic arrays," 2016 IEEE Electrical Power and Energy Conference (EPEC), Ottawa, ON, 2016, pp. 1-6.

[25] Abido, M. A., M. Sheraz Khalid, and Muhammed Y. Worku. "An efficient ANFIS-based PI controller for maximum power point tracking of PV systems." Arabian Journal for Science and Engineering 40.9 2641-265, 2015.

[26] Ammar A. Aldair, Adel A. Obed, Ali F. Halihal, "Design and implementation of ANFIS-reference model controller based MPPT using FPGA for photovoltaic system", Renewable and Sustainable Energy Reviews, Volume 82, Part 3 Pages 2202-2217, 2018.

[27]- Bezdec, J.C., Pattern Recognition with Fuzzy Objective Function Algorithms, Plenum Press, New York, 1981

[28] P. Naderi, "Distributed Generation, Using Battery/Photovoltaic System: Modeling and Simulation With Relative Controller Design," Journal of Solar Energy Engineering, vol. 135, no. 2, p. 6, 2013.

[29] May, Geoffrey J., Alistair Davidson, and Boris Monahov. "Lead batteries for utility energy storage: A review." Journal of Energy Storage 15: 145-157, 2018.

[30]] Anderson, Max D., and Dodd S. Carr. "Battery energy storage technologies." Proceedings of the IEEE 81.3: 475-479, 1993.

[31] S. Y. Mosazadeh, S. H. Fathi, M. Hajizadeh, and A. R. Sheykholeslami, "Adaptive hysteresis band controlled grid connected PV system with active filter function," International Conference on Power Engineering and Renewable Energy, pp. 1-6, 2012.

[32] Fen Tang, Xiao Zhou, Lexuan Meng,, Josep M. Guerrero and Juan C. Vasquez, , "Secondary Voltage Unbalance Compensation for Three-Phase Four-Wire Islanded Microgrids, 11th International Multi-Conference on Systems,Signals and Devices.